Applied Surface Science Advances 7 (2022) 100191

Contents lists available at ScienceDirect

Applied Surface Science Advances

journal homepage: www.sciencedirect.com/journal/applied-surface-science-advances

High-temperature oxidation and erosion of HVOF sprayed NiCrSiB/Al_2O_3 and NiCrSiB/WC—Co coatings

Ayyappan Susila Praveen [a], Arun Arjunan [b,*]

[a] Department of Mechanical Engineering, Vel Tech Rangarajan Dr. Sagunthala R&D Institute of Science and Technology, Tamil Nadu, India
[b] Additive Manufacturing of Functional Materials (AMFM) Research Group, School of Engineering, University of Wolverhampton, Telford Innovation Campus, TF2 9NT, United Kingdom

ARTICLE INFO

Keywords:
Ni-based
Coating, HVOF
High-temperature
Oxidation
Erosion

ABSTRACT

Material deterioration due to erosion and oxidation in high-temperature environments is a major cause of wear in power plants, aircraft engines and petrochemical industries. NiCrSiB based surface coatings using thermal spray techniques such as High-Velocity Oxy-Fuel (HVOF) offer a cost-effective route to improve the tribological properties for a range of substrate materials. The study investigates the high-temperature oxidation and erosion resistance of HVOF coated NiCrSiB reinforced with Al_2O_3 and WC—Co on SS304 stainless steel substrate. The oxidation kinetics and erosion responses of the coatings at 750 °C were evaluated for a period of 160 hrs and the coating microstructure, morphology and chemical compositions characterised. A total of three coating compositions were studied namely: NiCrSiB/Al_2O_3, NiCrSiB/n-Al_2O_3 and NiCrSiB/WC—Co where the results indicate a superior oxidation and erosion resistance in all cases in comparison to uncoated SS304. However, it was found that the NiCrSiB reinforced with micro-structured Al_2O_3 outperformed all the other coatings in terms of oxidation resistance. When it comes to erosion resistance, NiCrSiB/WC—Co was found to demonstrate the highest performance.

1. Introduction

Deterioration of tribological performance in high-temperature environments such as the ones in boilers and super-heaters is a significant problem that leads to premature failure. This leads to financial loss and machinery downtime for a range of industries adding significantly to their operating cost [1–3]. Generally, the most influential tribological properties that dictate the high-temperature wear of materials is their erosion and oxidation resistance [4,5]. According to Szymański et al. [6], a significant proportion of failure in boilers tubes that need immediate replacement is due to high-temperature erosion. This is a result of fly ash erosion caused because of impinging carbon and the oxide particles carried by the flue-gas post-combustion adding as much as 54% of the total maintenance cost according to Cheng et al. [7]. Developing suitable coatings that offer high oxidation and erosion resistance is the most cost-effective method in addressing the problems.

Although there are several surface coating techniques as summarised in Fig. 1, thermal spraying is considered the most versatile as it can be used to spray both ceramic and metallic feedstock to a targeted substrate [8–10]. The HVOF techniques make use of fuel and oxygen combustion to generate high pressure and temperature environment that is used to spray powdered feedstock [11]. Due to the high temperature and pressure, the feedstock material partially melts during the coating process improving both the surface finish and density [12,13]. The HVOF coating process generally features a flame temperature around 3000 K while preserving high particle velocity making them suitable to spray coatings with low porosity and high hardness which are often favourable [14–16].

One of the most cost-effective approaches to improve the tribological performance of surfaces exposed to a high-temperature environment is the deposition of nickel (Ni) based coatings. Nickel-chromium-silicon-boron (NiCrSiB) coatings are known to improve tribological properties such as wear, oxidation and corrosion resistance due to their superior mechanical properties and low environmental impact [17–20]. While Ni is the major constituent that provides strength, Cr enhances high-temperature (850 °C) oxidation resistance, Si improves type II hot corrosion resistance and B influences the formation of hard phases in the Ni matrix. Overall, the combination results in achieving good wear and oxidation resistance for a range of applications. Furthermore, boron and silicon reduce the overall melt temperature which introduces

* Corresponding author.
E-mail address: a.arjunan@wlv.ac.uk (A. Arjunan).

https://doi.org/10.1016/j.apsadv.2021.100191
Received 5 August 2021; Received in revised form 10 October 2021; Accepted 26 October 2021
Available online 2 November 2021

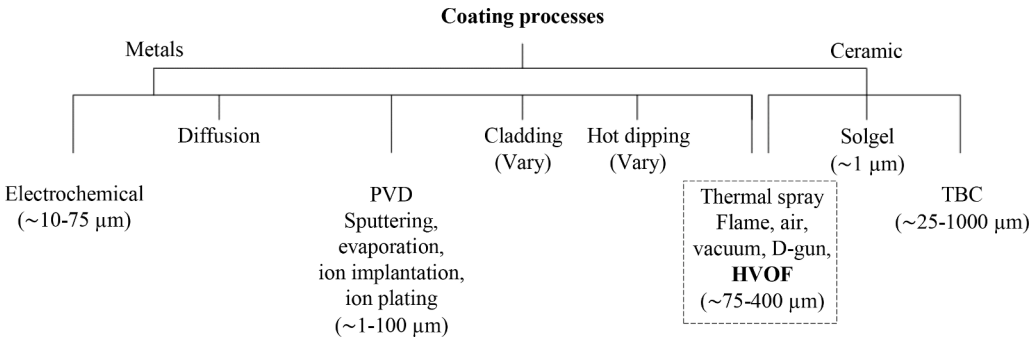

Fig. 1. Some of the common surface coating techniques used for metals and ceramics were the HVOF technique offers the most flexibility highlighted as suitable for both metals and ceramics. The abbreviations used in the figure read Physical vapor Deposition (PVD), Thermal Barrier Coatings (TBC) and Detonation Gun (D-gun).

Table 1
Composition (*wt.*%) of SS304 substrate used for HVOF coating.

Element	C	Mn	Si	Cr	Ni	P	S	Fe
Composition	0.023	1.440	0.366	18.736	8.288	0.029	0.006	Bal.

Table 2
Characteristics of the primary matrix and reinforcing elements used as HVOF feedstock.

Material	Composition (*wt.*%)	Particle size	Manufacturing
NiCrSiB	Ni-72, Cr-16, Si-5, B-3	53 μm	Gas atomized
Al_2O_3	Al_2O_3 (99)	45 μm	Fused and crushed
n-Al_2O_3	Al_2O_3 (99)	45 nm	Mechanically alloyed
WC—Co	WC (88), Co (12)	15 μm	Agglomerated, sintered

self-fluxing characteristics leading to improved density [21,22].

Studies attempting to improve high-temperature erosion include investigations on NiCrAlY coating [23] yielding superior performance even at 540 °C up to 100 hrs. Lopez et al. [24] employed HVOF to coat equal amounts (50:50) of powdered Ni and Cr feedstock on a steel substrate resulting in tenfold improvement in high-temperature (550 °C and 650 °C) erosion between the coated and uncoated sample post-360 hrs. Research by Bala et al. [25] used Ni and Cr in varying proportions (50:50 and 50:20 *wt.*%) deposited using cold spray on steel and studied its performance at 900 °C. The results showed both the coatings to offer increased resistance to oxidation in comparison to the uncoated substrate with a 50% reinforcement of Cr with Ni outperforming the 20% Cr variant.

Modifying alloying compositions are increasingly being experimented in an attempt to improve the high-temperature performance of Ni-based coatings. As such coatings that feature microstructured and nanostructured hard phases such as tungsten carbide (WC), cobalt-chromium (CoCr), aluminium oxide (Al_2O_3) and chromium carbide (Cr_3C_2) are all reinforcing with Ni [26–32]. Studies on Al_2O_3 addition in literature [26,33,34] demonstrate microstructure refinement showing phase characteristics suitable for enhanced wear and microhardness and related tribological properties. HVOF sprayed coatings reinforced with tungsten carbide-cobalt (WC—Co) reinforcement by Yuan et al. [35] also showed a significant improvement in both wear and micro-hardness properties.

Although some of the existing studies validate the potential use of Al_2O_3 and WC—Co when it comes to tribological coatings, their use as reinforcement agents in NiCrSiB to improve high-temperature oxidation and erosion resistance are yet to be established. A critical aspect in this regard is also to identify the influence of these reinforcements on the oxidation kinetics under high-temperature environments. Accordingly, this study evaluates the oxidation and erosion performance of HVOF deposited NiCrSiB compositions reinforced with Al_2O_3 its nanostructured variant (hereafter referred to as n-Al_2O_3) and WC—Co on SS304 stainless steel substrate exposed to a high-temperature environment.

2. Materials and methods

2.1. Base material and coating composition

Although the feedstock used in HVOF are solid they are either molten or semi-molten by the time they are deposited on the substrate surface depending on the functional requirement and the coating parameters used. As such the properties of both the substrate and the powder feedstock are a critical factor for a successful coating process. Generally, SS304, SS310 and SS316 steels are used for high-temperature (600 °C) applications involving erosion and corrosion damages [36]. Therefore, SS304 steel having a chemical composition summarised in Table 1 was the coating substrate of choice since high-temperature performance is being assessed.

Pre-processing routine for the substrate involved roughening the surface using a suction blasting machine featuring 320–500 μm corundum grits. Surface roughening is an essential step that is required for any coating application as it increases the surface roughness of the coated surface leading to enhanced mechanical interlocking at the coating interface [37]. Post-roughening, acetone bath was used to clean the samples; subsequently, the surface roughness was characterised and found to be consistent at 8–10 μm between all the substrate samples used.

There is a significant demand for coatings with improved high-temperature oxidation erosion performance for a wide range of industries. Ni alloys offer significant potential in this regard due to their superior erosion behaviour. Although numerous Ni variants exist, NiCrSiB offers a significant advantage due to the existence of borides and carbides [38,39]. Borides are known to have superior hardness and high melting point; a combination that makes them particularly suitable for high-temperature environments. Carbides on the other hand feature exceptional wear resistance making them suitable to be employed in high erosion environments. Altogether, atomised NiCrSiB composition reinforced with Al_2O_3, and WC—Co seems to offer significant potential to be investigated for high-temperature erosion and oxidation applications. All coating compositions and their nominal particle sizes are summarised in Table 2. The micron sized powders NiCrSiB (MEC-335), Al_2O_3 (MEC-740) and WC—Co (MEC-518) were procured from M/s. Metallizing Equipment Co. Pvt. Ltd (MEC), Jodhpur, India. The

Table 3
Process parameters used for the HVOF spraying technique of the coatings.

Parameter	NiCrSiB/ Al_2O_3	NiCrSiB/n- Al_2O_3	NiCrSiB/ WC—Co
Fuel flow rate (LPM)	65±0.5	60±0.5	65±0.5
Oxygen flow rate (LPM)	260±0.5	250±0.5	220±0.5
Powder feed rate (g/min)	28±0.1	28±0.1	28±0.1
Standoff distance (mm)	250±5	250±5	300±5
Feedstock ratio (*wt.*%)	60/40	98.6/1.4	65/35

Table 4
Parameters used for high-temperature erosion testing using hot jet erosion technique.

Parameter	Value
Erodent	Alumina
Particle size	50 μm
Velocity	40 m/s
Feed rate	5 g/min
Angle of impact	30 °, 60° and 90°
Test temperature	750 °C
Duration	10 min.
Nozzle dia.	1.5 mm
Standoff distance	10 mm

nano-Al_2O_3 (44,931) powder was supplied by Alfa Aesar. The nominal particle size distribution of the feedstock was characterised using the well-established laser diffraction technique using a Malvern Mastersizer 2000 (UK) following ASTM C1070. Water was used as the medium for laser diffraction test. The nanostructured version NiCrSiB/n-Al_2O_3 was also considered to evaluate the significance of particle size distribution and packing density on the oxidation erosion performance. The NiCrSiB/Al_2O_3 and NiCrSiB/WC—Co composites powders were prepared using a turbo mixer for 1 h in order to obtain homogeneous mixing. The mechanical alloying of the NiCrSiB/n-Al_2O_3 feedstock powder mixture was carried out using a ball mill featuring a planetary arrangement of 250 ml hardened steel vial and 10:1 powder to ball weight ratio at 250 rpm. In order to prevent excessive cold welding during the mechanical alloying process ethanol was used as the process control agent (PCA). Typically, ethanol is absorbed at the surfaces of the powdered particles and aids in reducing excessive cold welding between the powders along with the grinding medium and the milling container. This subsequently reduces agglomeration of particles which affects both flowability and the packing density. The mechanical alloying of NiCrSiB/n-Al_2O_3 powder mixtures considered in this study were carried out in normal atmospheric conditions.

2.2. HVOF process parameters

Three Ni-based coatings NiCrSiB/Al_2O_3, NiCrSiB/n-Al_2O_3 and NiCrSiB/WC—Co were deposited onto the SS304 base material using HVOF thermal spraying system. The HVOF techniques use a carrier-gas to introduce the feedstock into the high pressure and temperature environment that is being generated because of oxy-fuel combustion. As such the powdered feedstock get semi-molten which is subsequently deposited onto the coated surface using a high-velocity nozzle at a standoff distance [40]. The HVOF thermal spraying was carried out using the HIPOJET 2700 system (Make: Metallizing Equipment Co. Jodhpur, India). The fuel gas used was Liquified Petroleum Gas (LPG). The studies indicated that the HVOF process parameters such as fuel and oxygen flow rate along with feedstock rate and standoff distance affect the properties of the coating. Optimum process parameters were evaluated for each of the composition, which is as summarised in Table 3 that was subsequently used for the coating deposition [9,41]. The thickness of all coatings was characterised and controlled to within 250±20 μm for systematic comparison.

2.3. Characterisation

The phases that were present both in the coating composition and the coated surfaces were analysed using X-ray Diffractometer (XRD). The samples for cross-sectional analysis were prepared by slicing the coated substrate and hot-press mounting in resin. The coating morphology was analysed using both scanning electron microscopy (SEM) and the Energy Dispersive X-ray Spectroscopy (EDS) made by Hitachi and Bruker, respectively. The porosity of the coating was analysed from the cross-sectional SEM images. The resulting data were further processed using 'ImageJ processing and analysis software' to calculate the percentage value of porosity. A total of ten different measurements were taken at different locations and the average results are presented. The technique is widely used [42] to evaluate representative porosity data from cross-sectional SEM images. The Vickers microhardness machine (Wilson Hardness tester-402 MVD) at 300 g load at 15 s was used for micro-hardness characterisation.

2.4. High-temperature testing

2.4.1. Oxidation

The evaluation of oxidation performance at high temperature was carried out in an electric tubular furnace at 750 °C for a duration of 160 h. The testing temperature was selected to match the typical working temperature of boiler tubes. The dimensions of the coated specimens were measured using a digital Vernier calliper to calculate the surface area of samples. Before oxidation evaluation, all samples were acetone cleaned and 80 °C oven-dried for two hrs. The alumina crucibles were heat-treated at 900 °C for a duration of 4 h to avoid the influence of volatile matter and ensure constant weight throughout the study. The specimens were kept in an alumina crucible and weighted at an accuracy of 1×10^{-4} g before being placed in the hot zone of the furnace maintained at 750 °C. The mass changes of the samples were measured at 20 hr regular intervals.

2.4.2. Erosion

The characterisation of the erosion performance was carried out following ASTMG76–02 [43] in a hot-air-jet erosion machine. The tests were conducted at varying angles of 30°, 60° and 90° to characterise the erosion mechanism of the coatings. The major problems to be solved in power generations plants are high-temperature oxidation and erosion by the impact of fly ashes and unburned carbon particles especially in the regions where the component surface temperature is above 600 °C. Also, low temperature hot corrosion occurs at a temperature about 700 °C-750 °C on the fireside boiler tubes in coal-fired steam generating plant [44]. This work aims to understand the erosion and oxidation resistance of thermal sprayed NiCrSiB/Al_2O_3 and NiCrSiB/WC—Co coatings under conditions as close as possible to those experienced within a power plant boiler tube. So, the erosion experiments were carried out at 750 °C to mimic a high-temperature erosion environment that is representative of industrial environments. The parameters used for the erosion test experiments are summarised in Table 4. Two sets of erosion tests were carried out for each coating composition being analysed to ensure repeatability of the results. Post-testing the eroded samples were unmounted and cleaned with acetone before characterising material loss. Using the data, the rate of erosion was calculated as the ratio of the mass of material eroded (g) to that of the erodent particle (g) used.

3. Results and discussion

3.1. Microstructure and properties

The morphology of the feedstock powders used for the HVOF are shown in Fig. 2. NiCrSiB is spherical while micron sized Al_2O_3 feature an angular morphology. In comparison the WC—Co feedstock is near

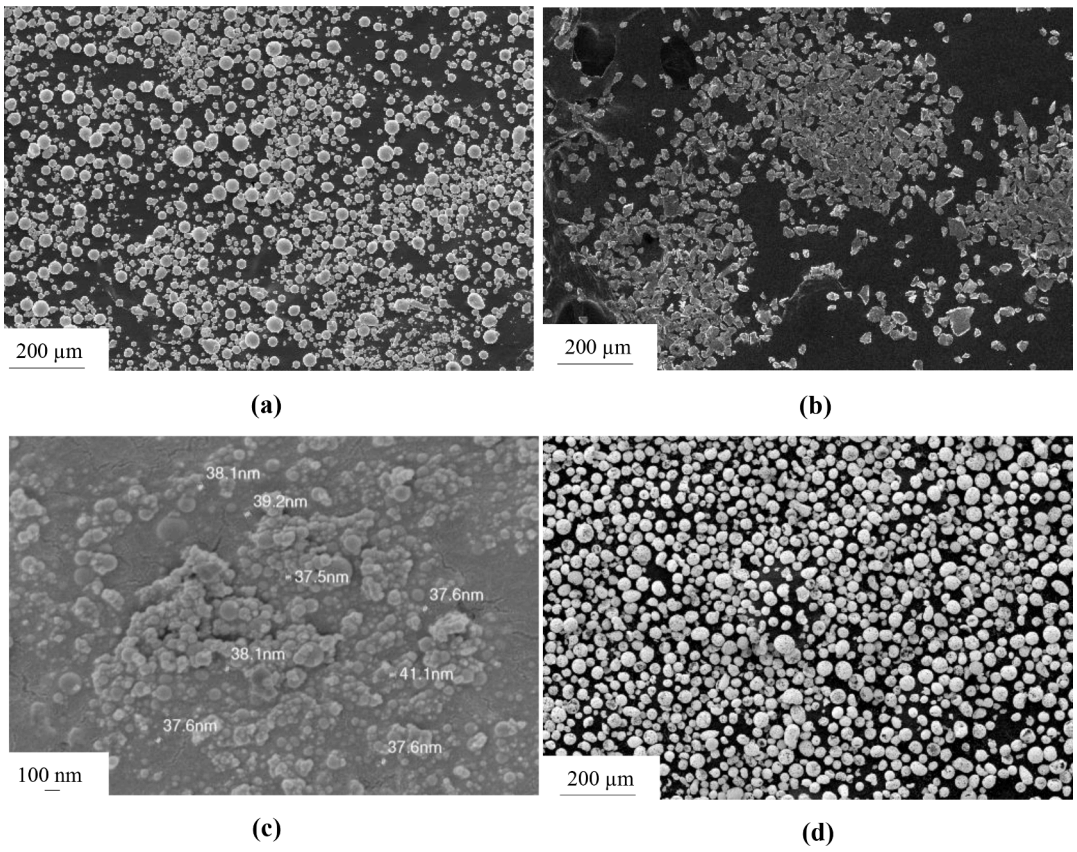

Fig. 2. Morphology of the feedstock particles considered for the study showing (a) NiCrSiB, (b) micron-sized Al_2O_3 (c) nano-sized Al_2O_3 and (d) WC—Co.

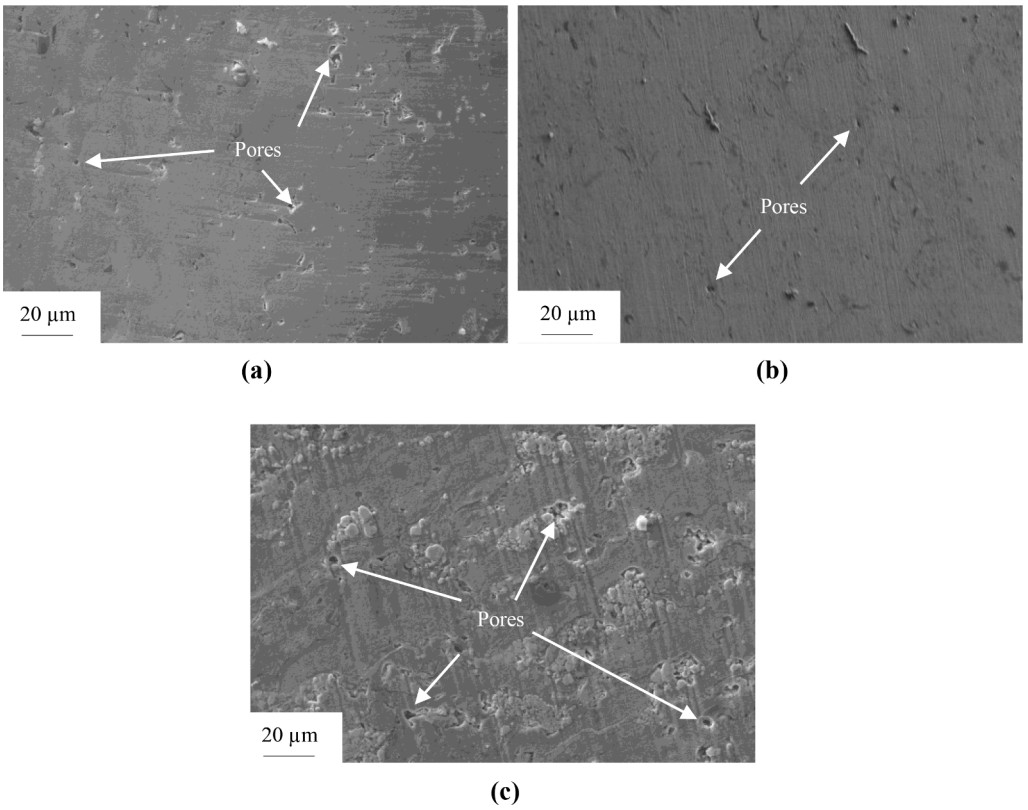

Fig. 3. Cross-section of the as coated samples evaluated using scanning electron microscopy showing (a) NiCrSiB/Al_2O_3, (b) NiCrSiB/n-Al_2O_3 and (c) NiCrSiB/WC—Co.

Table 5
Characteristics of the reinforced coatings deposited using HVOF in comparison to NiCrSiB.

Descriptions	NiCrSiB/Al_2O_3	NiCrSiB/n-Al_2O_3	NiCrSiB/WC—Co
Porosity (%)	1.5 ± 0.4	1.2 ± 0.4	1.8 ± 0.65
Surface roughness (μm)	9.3 ± 2.4	8.5 ± 1.5	8.5 ± 1.5
Microhardness ($HV_{0.3}$)	843±94	748±80	928±108

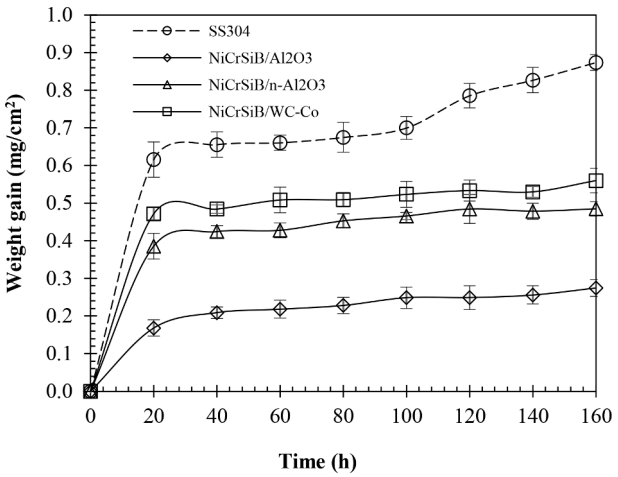

Fig. 4. Experimentally evaluated high-temperature oxidation responses for the HVOF coatings.

spherical with micro-pores architecture. The micro-pores architecture is generally considered advantageous for the thermal spray processing as they contribute to homogenous heating of the feedstock during powder particle-flame interaction. Fig. 2c shows the morphology of nano- Al_2O_3 indicating a spherical morphology with a wide range of particle sizes.

The cross-sections of the samples were analysed as shown in Fig. 3 to understand the internal structure and composition of the coatings that were generated. Three coating cases were considered namely: NiCrSiB/Al_2O_3, NiCrSiB/n-Al_2O_3 and NiCrSiB/WC—Co. All three coatings showed lamellar structure representative of the HVOF coatings with occasional un-melted particles and porosity voids because of oxide inclusion. From Fig. 3b the NiCrSiB reinforced with Al_2O_3 nanoparticles (n-Al_2O_3) results in a uniform coating with less porosity which demonstrates the effectiveness of packing density in the resulting density of the coating.

In comparison, the morphology of the coating in Fig. 3a shows the existence of high porosity and un-melted Al_2O_3 particles. The melting temperature of aluminium oxide is 2100 °C which is significantly higher than that of nickel, as such the composition featuring a higher percentage of nickel can melt more effectively. Therefore, the composition that features nanoparticles of aluminium oxide can absorb sufficient heat that results in a coating of higher density. The number of pores observed was comparatively less when reinforced with nanoparticles of aluminium oxide in comparison to the other two cases: an effect attributable to the percentage of nanostructured aluminium oxide in the feedstock. When it comes to NiCrSiB/WC—Co coating, Fig. 3c shows the presence of nickel (grey) and tungsten carbide (brighter fields) in the microstructure. Overall, for all cases, the coatings show splats formed of partially melted particles representative of thermal spray coatings.

The most common performance indicators for the as coated surface are summarised in Table 5. When compared to the substrate microhardness of 180 $HV_{0.3}$, all the HVOF coatings were found to exhibit superior performance. The highest microhardness was observed for NiCrSiB/WC—Co coating which was an increase of 61% compared to the exposed substrate. Out of the three coatings investigated, the lowest performance was exhibited by NiCrSiB/n-Al_2O_3 at a hardness of 748 $HV_{0.3}$ which is still a 30% improvement in comparison to the uncoated surface. The increase in hardness is a result of the work-hardening effect in steel due to the HVOF feedstock impact. This phenomenon is not typical of thermal spray and was also observed [45,46] when using cold spray coating.

When it comes to surface roughness, the highest average roughness was exhibited by NiCrSiB/Al_2O_3 at a surface roughness of 9.3 μm; a 9% increase in comparison to the other two coatings tested. However, comparing the results of NiCrSiB/Al_2O_3 and NiCrSiB/n-Al_2O_3, the increase in surface roughness is a result of Al_2O_3 particle size. This is also the result why a nanoparticle addition and WC—Co resulted in similar surface roughness at 8.5 μm. Overall, the surface roughness of the HVOF coatings studied was found to be similar to those reported in the literature for alternative coatings deposited using the HVOF technique [18, 47–49].

3.2. *High-temperature oxidation*

3.2.1. *Oxidation kinetics*

Oxidation kinetics is a critical parameter in characterising the performance of a coating where it refers to the variation of oxidation rate with time. Fig. 4 shows the mass gain per unit area of the SS304 substrate along with NiCrSiB/Al_2O_3, NiCrSiB/n-Al_2O_3 and NiCrSiB/WC—Co coatings during oxidation at 750 °C at different time intervals up to 160 hrs. For the uncoated substrate (SS304), the mass gain was found to increase at a higher rate with an increase in the oxidation time. Nevertheless, the oxidation behaviour of all the three HVOF sprayed coatings can be seen (Fig. 4) to be different in comparison with the substrate.

As shown in Fig. 4, the mass gain of the SS304 sample was found to

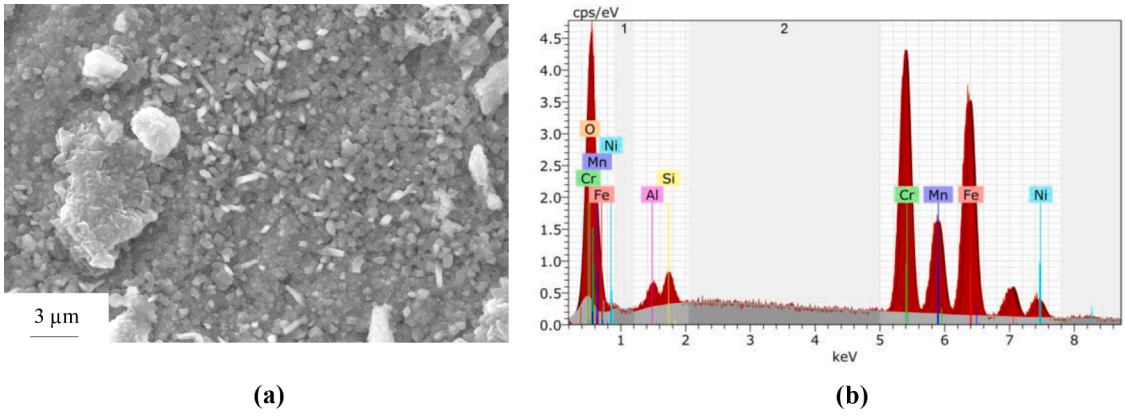

Fig. 5. SEM data of the oxidated SS304 substrate showing (a) the post-oxidation surface topography and (b) EDS elemental spectrum.

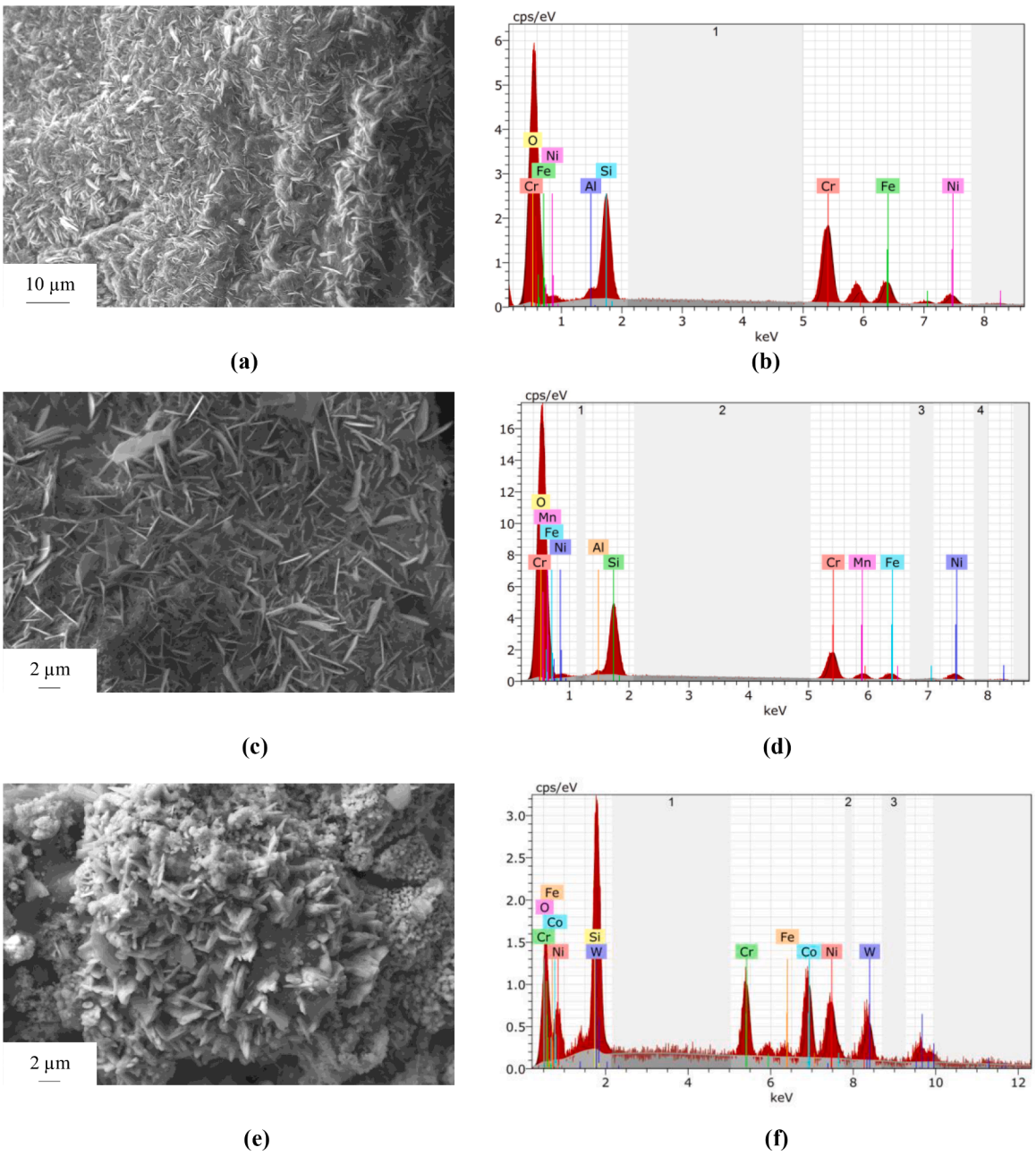

Fig. 6. Surface topography and elemental spectrum of the oxidised coatings showing (a) NiCrSiB/Al_2O_3 surface and (b) corresponding elemental composition, (c) NiCrSiB/n-Al_2O_3 surface and (d) corresponding elemental composition, (e) NiCrSiB/WC—Co surface and (f) corresponding elemental composition.

Table 6
Composition of the coated and uncoated samples post-oxidation showing *wt.*% of elemental distribution.

Description	Si	Fe	Ni	Cr	O	Al	Mn	W	Co	Total
SS304	1.99	31.29	3.60	25.48	28.08	2.21	7.36	–	–	100
NiCrSiB/Al_2O_3	17.69	10.05	5.29	25.88	38.62	2.47	–	–	–	100
NiCrSiB/n-Al_2O_3	20.89	6.76	7.14	21.47	39.75	1.65	2.34	–	–	100
NiCrSiB/WC—Co	4.34	1.11	13.48	12.73	14.81	–	–	35.69	17.85	100

be four times higher than that of HVOF sprayed NiCrSiB/Al_2O_3. The oxide scales formed on the steel surface were completely detached and with high porosity incapable of protecting the base material from continuous oxidation in an effective manner. During the entire length of the test, the oxidation behaviour continued to worsen concerning time, as indicated in Fig. 4. The highest increase in mass in the first measure period (20 hrs) is a result of the rapid oxygen pick up through diffusion consistent with the literature [50,51].

Post-20 hrs of oxidation, the oxidative mass gain of the coated samples increased rapidly which indicates rapid oxide formation at the surface, splat boundaries and open pores due to the penetration of the oxidizing species along the splat boundaries. Post-oxide formation within pores and splat boundaries, the coating becomes dense and the diffusion of oxidising species to the internal portion of the coatings slows

Table 7
Compound formation deduced from EDS profiling of the respective coated and uncoated samples post-oxidation showing *wt.*% elemental compounds.

Description	FeO	Cr_2O_3	MnO	NiO	Al_2O_3	SiO_2
SS304	40.26	37.23	9.50	4.58	4.17	4.25
NiCrSiB/Al_2O_3	12.93	37.82	–	6.74	4.67	37.84
NiCrSiB/n-Al_2O_3	6.69	31.38	3.02	9.09	3.13	44.70
NiCrSiB/WC—Co	1.43	18.60	–	17.15	–	9.28

down. Subsequently, the growth of the oxides become largely limited to the surface leading to a steady rate of oxidation in conjunction with exposure time. Nevertheless, the slow rate of weight gain during the subsequent cycles implies mass loss due to the oxidation of carbon.

Overall, the HVOF sprayed NiCrSiB/Al_2O_3 coatings exhibited the lowest weight gain in comparison to both NiCrSiB/n-Al_2O_3 and NiCrSiB/WC—Co coatings. The reasons for the improved oxidation resistance for the NiCrSiB/Al_2O_3 coating is the existence of dense, slow-growing and thermodynamically stable Al_2O_3 which hinders the diffusion of oxygen (or metal ions) slowing down the oxide growth rate. The presence of Al_2O_3 $_s$ phase in the NiCrSiB matrix also hinders the diffusion of Ni and Cr while reducing the growth of Cr_2O_3 and $NiCr_2O_4$ due to the low diffusion coefficient of nickel and chromium in Al_2O_3 [52]. Thus, the Al_2O_3 $_s$ phase gives priority to the growth of protective oxide during oxidation. In comparison, the uncoated SS304 substrate showed a maximum mass gain of 0.87 mg/cm^2 and the NiCrSiB/Al_2O_3 coating exhibited a minimum mass gain of 0.27 mg/cm^2. The mass gain of NiCrSiB/n-Al_2O_3 (0.48 mg/cm^2) and NiCrSiB/WC—Co (0.56 mg/cm^2) were more than NiCrSiB/Al_2O_3 coating but less than the SS304 sample. Therefore, it is evident that the increase in mass of SS304 can be significantly reduced using the HVOF coatings.

3.2.2. *Surface analysis*

To understand the composition and morphology of the samples post-oxidisation, the surfaces were characterised using EDS. Analysing the uncoated sample (Fig. 5a) indicate that SS304 was severely damaged because of oxidation through the scale spallation mechanism. The EDS data revealed that iron, chromium, and oxygen as the major constituents in the oxidized SS304 sample (Fig. 5b). The presence of ferric oxide (Fe_2O_3) in the scales of the oxidized sample indicated non-protective surface conditions consistent with the literature [53].

Figs. 6 shows the surface morphologies of HVOF sprayed NiCrSiB/Al_2O_3 (Fig. 6a), NiCrSiB/n-Al_2O_3(Fig. 6c), and NiCrSiB/WC—Co (Fig. 6e) coatings after oxidation test at 750 °C for 160 h. The respective oxidation products on the surface of the coatings were evaluated using the EDS technique as shown in Fig. 6b, 6d and 6e with the resulting elements presented in Table 6 and compounds in Table 7. The EDS analysis revealed that the major oxidation products were in the form of chromium oxide as listed in Table 7. From Fig. 6a and 6c, the tiny oxide particles were mainly flaky in shape. The mass gain of HVOF sprayed NiCrSiB/Al_2O_3 was about 43% and 51% less than that of HVOF sprayed NiCrSiB/n-Al_2O_3 and NiCrSiB/WC—Co coatings after 160 h of oxidation.

When NiCrSiB was reinforced with tungsten carbide cobalt, the oxidation resistance reduced in comparison with the NiCrSiB/Al_2O_3 coating. This may be attributed to the higher oxidation rate of WC in the coating. During the oxidation test in the temperature range of 700–800 °C, NiO was found to increase significantly as listed in Table 7 in comparison to the other coatings similar to the case observed in the studies carried out by Kunioshi et al. [54]. The EDS analysis of the oxidised NiCrSiB/WC—Co coatings summarised in Table 6 and 7 further confirms the above aspect. Overall, the higher oxidation resistance of NiCrSiB reinforced in aluminium oxide coating is due to the formation of protective oxides of chromium (Cr_2O_3), aluminium (Al_2O_3) and nickel

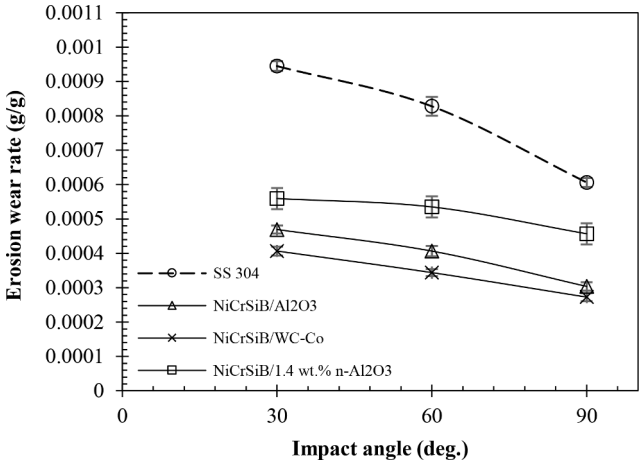

Fig. 8. Comparison of high-temperature erosion wear rate of all the coatings and SS304 substrate at 750 °C.

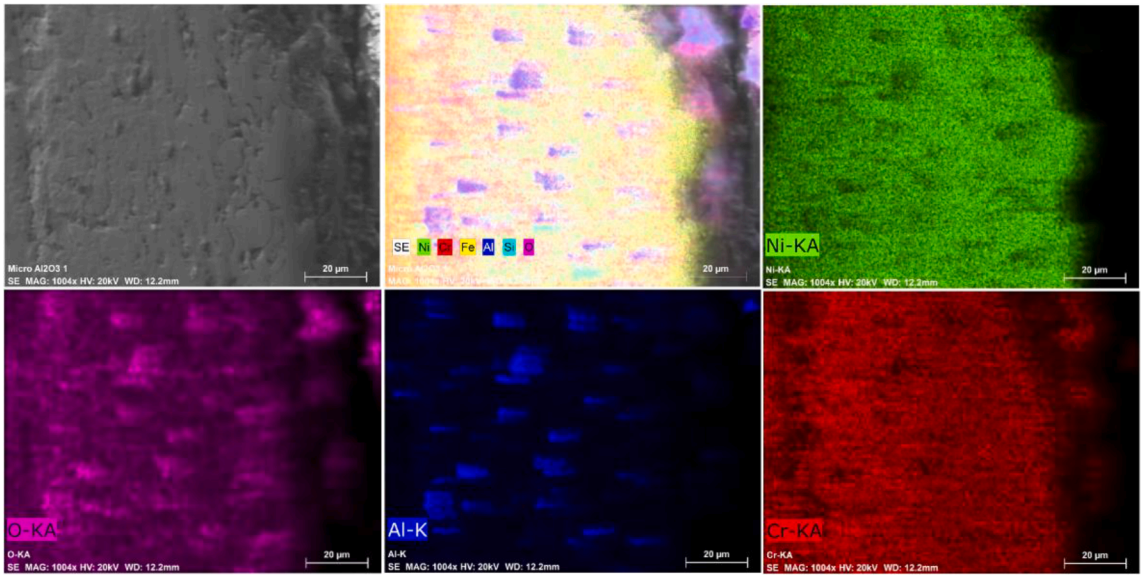

Fig. 7. Cross-sectional mapping of the best performing coating composition (NiCrSiB/Al_2O_3) that showed the highest oxidation resistance.

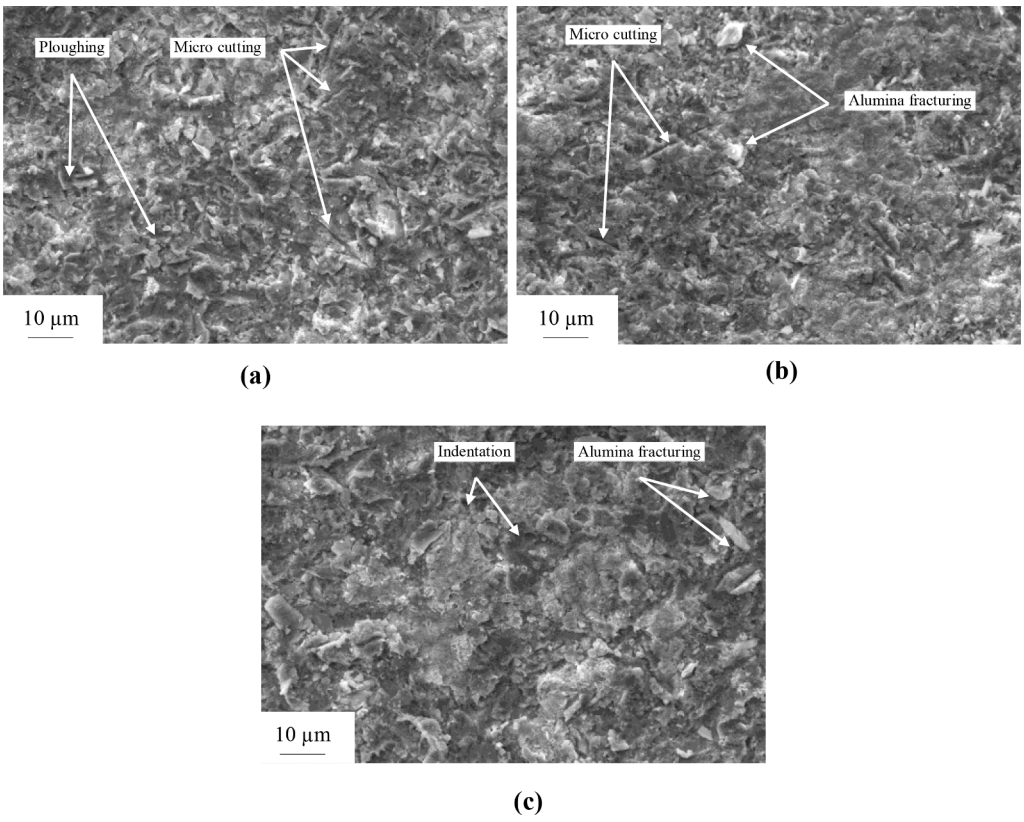

Fig. 9. SEM image of the high-temperature (at 750 °C) eroded surface of the best performing coating (NiCrSiB/WC-Co) coating at (a) 30° (b) 60° and (c) 90° impact angle.

(NiO) which was confirmed through the EDS analysis.

The higher presence of chromium oxide was also observed from the X-ray mapping as shown in Fig. 7, which aids in shielding the base metal against any diffusion of the oxidizing species. The Cr_2O_3 phase is thermodynamically stable [55] resulting in a dense, continuous layer (Fig. 6c). This result in a solid diffusion barrier that prohibits oxygen interaction with the coating material underneath. The added presence $NiCr_2O_4$ in the oxide scales also aids in the development of higher oxidation resistance in the NiCrSiB coating reinforced with aluminium oxide. From the EDS analysis (Fig. 6 and Table 7), it can be seen the percentage of Cr_2O_3 in NiCrSiB/Al_2O_3 is high in comparison to NiCrSiB/n-Al_2O_3. As a result, the coating composition featuring NiCrSiB/Al_2O_3 outperforms its nano counterpart.

3.3. High-temperature erosion

High-temperature erosion affects a range of industries increasing maintenance periods costing time and reduced efficiency. In most cases, especially in the power generation sector oxidation and erosion ranks top in their order of influence of material failure. However, the worst-case scenarios are due to the combined effect of erosion and oxidation. To understand the interactions between the two processes it is necessary to understand both the oxidation behaviour and high-temperature erosion of the coatings being considered. As such Fig. 8 shows the rate of erosion wear of the NiCrSiB coatings reinforced with Al_2O_3, WC—Co, and n-Al_2O_3.

It was found that the erosion rate of all the coatings decreased with an increase in the erodent angle at 750 °C indicative of the ductile mode of erosion mechanism at high temperature. This may be due to the presence of metallic phases over the surface of the coatings. In general, three erosion rate responses have been noted with an increase in temperature. Generally, when materials are exposed to temperatures above 400 °C, they show a decrease in erosion resistance consistent with an increase in temperature [56]. As an aspect reported by Gat and Tabakoff [57] who evaluated the erosion response in terms of the effect of temperature on material properties and found that an increase in temperature decreased the erosion resistance.

The SEM images of the eroded best performing coating (NiCrSiB/Al_2O_3) at different impact angles are shown in Fig. 9, where the erosion resistance of the NiCrSiB/WC—Co was 13%, 27% and 57% higher than that of HVOF sprayed NiCrSiB/Al_2O_3 and NiCrSiB/n-Al_2O_3 coatings and SS304 substrate respectively, at an impact angle of 30°

Evaluating the microscopy data as shown in Fig. 9, the micro-cutting and plough indentation were found to be higher when the erodent angle was at the lowest angle (Fig. 9a). Normally, such a phenomenon is a result of the higher shear stress (τ) [45]. In comparison, if the erodent angle is perpendicular (90°) to the coating surface, the collision causes craters representative of a compressive ($-\sigma$) failure. Although, the extrusion of material around the plastic deformation indicates a soft-bound matrix, the characteristics indicate the ductile mode of erosion. Generally, when developing coatings for industrial application, ductile erosion is favourable as it reduces catastrophic failure due to crack propagation, unlike brittle erosion.

The HVOF NiCrSiB coating reinforced with tungsten carbide cobalt showed the least erosion wear rate of 0.000273 g/g whereas the SS304 uncoated sample exhibited the highest erosion wear rate of 0.000606 g/g when exposed to perfectly axial erodent (90°). The higher erosion resistance of the NiCrSiB/WC—Co coatings can be attributed to the higher hardness and fracture toughness value of WC—Co as compared to Al_2O_3. The HVOF sprayed NiCrSiB/WC—Co coating exhibited a high hardness value of 928 $HV_{0.3}$ as compared to NiCrSiB/Al_2O_3 coating (843 $HV_{0.3}$). The toughness value of the WC—Co ranges from 4 to 6 MPa $m^{-1/2}$ consistent with the observations of Chivavibul et al. [58] whereas for Al_2O_3 it is between 1 and 2 MPa $m^{-1/2}$ consistent with Grewal et al. [26]. Overall, for all the coatings and substrate materials tested the highest erosion was observed at 30° and lowest at 90° indicating a lower

shear strength in comparison to compression.

4. Conclusions

The study evaluated the high-temperature oxidation and erosion behaviour of HVOF NiCrSiB/Al_2O_3, NiCrSiB/n-Al_2O_3 and NiCrSiB/WC—Co coatings on an SS304 steel substrate. The results showed that the HVOF coating technique results in the formation of high-density NiCrSiB/Al_2O_3, NiCrSiB/n-Al_2O_3 and NiCrSiB/WC—Co coatings with low porosity and high hardness. However, the high-temperature oxidation and erosion performance of the coatings were observed to be different. It was found that the high-temperature oxidation performance of NiCrSiB/Al_2O_3 coatings was superior to that of NiCrSiB/WC—Co coatings due to the presence of protective oxide layers like Cr_2O_3, Al_2O_3, $NiCr_2O_4$ and NiO. The oxidative mass gain of HVOF sprayed NiCrSiB/Al_2O_3 coating was less than that of NiCrSiB/n-Al_2O_3 and NiCrSiB/WC—Co by 43% and 51% respectively post-160 hrs oxidation period. The decrease in oxidation resistance of the NiCrSiB/WC—Co coating was attributed to the high oxidation rate of WC at high temperatures and the increase in WO_3 content. When it comes to high-temperature erosion performance, NiCrSiB/WC—Co coating outperformed both NiCrSiB/Al_2O_3 and NiCrSiB/n-Al_2O_3 coatings by demonstrating the highest erosion resistance. The superior performance was attributed to the better fracture toughness and hardness value of the WC—Co as compared to Al_2O_3. The high-temperature (750 °C) mode of erosion was found to be ductile due to the presence of a large number of metallic phases over the coated surface.

Declaration of Competing Interest

The authors declare that they have no known competing financial interests or personal relationships that could have appeared to influence the work reported in this paper.

References

[1] S. Matthews, B. James, M. Hyland, High temperature erosion–oxidation of Cr3C2–NiCr thermal spray coatings under simulated turbine conditions, Corros. Sci. 70 (2013) 203–211, https://doi.org/10.1016/j.corsci.2013.01.030.

[2] H. Vasudev, L. Thakur, A. Bansal, H. Singh, S. Zafar, High temperature oxidation and erosion behaviour of HVOF sprayed bi-layer Alloy-718/NiCrAlY coating, Surf. Coatings Technol. 362 (2019) 366–380, https://doi.org/10.1016/j.surfcoat.2019.02.012.

[3] M. Kaur, H. Singh, S. Prakash, Surface engineering analysis of detonation-gun sprayed Cr3C2–NiCr coating under high-temperature oxidation and oxidation–erosion environments, Surf. Coatings Technol. 206 (2011) 530–541, https://doi.org/10.1016/j.surfcoat.2011.07.077.

[4] G. Sundararajan, M. Roy, Solid particle erosion behaviour of metallic materials at room and elevated temperatures, Tribol. Int. 30 (1997) 339–359, https://doi.org/10.1016/S0301-679X(96)00064-3.

[5] V.H. Hidalgo, F.J.B. Varela, a.C. Menéndez, S.P. Martínez, A comparative study of high-temperature erosion wear of plasma-sprayed NiCrBSiFe and WC-NiCrBSiFe coatings under simulated coal-fired boiler conditions, Tribol. Int. 34 (2001) 161–169, https://doi.org/10.1016/S0301-679X(00)00146-8.

[6] K. Szymański, A. Hernas, G. Moskal, H. Myalska, Thermally sprayed coatings resistant to erosion and corrosion for power plant boilers - A review, Surf. Coatings Technol. 268 (2015) 153–164, https://doi.org/10.1016/j.surfcoat.2014.10.046.

[7] J.B. Cheng, X.B. Liang, Y.X. Chen, Z.H. Wang, B.S. Xu, High-Temperature Erosion Resistance of FeBSiNb Amorphous Coatings Deposited by Arc Spraying for Boiler Applications, J. Therm. Spray Technol. 22 (2013) 820–827, https://doi.org/10.1007/s11666-012-9876-5.

[8] L. Pawlowski, Thermal Spraying Techniques, Sci. Eng. Therm. Spray Coatings (2008) 67–113, https://doi.org/10.1002/9780470754085.ch3.

[9] A.S. Praveen, A. Arjunan, Parametric optimisation of High-Velocity Oxy-Fuel Nickel-Chromium-Silicon-Boron and Aluminium-Oxide coating to improve erosion wear resistance, Mater. Res. Express. (2019), https://doi.org/10.1088/2053-1591/ab301c.

[10] F. Ghadami, A.S.R. Aghdam, S. Ghadami, Abrasive wear behavior of nano-ceria modified {NiCoCrAlY} coatings deposited by the high-velocity oxy-fuel process, Mater. Res. Express. 6 (2020) 1250d6, https://doi.org/10.1088/2053-1591/ab63f4.

[11] A. Dolatabadi, V. Pershin, J. Mostaghimi, New attachment for controlling gas flow in the HVOF process, J. Therm. Spray Technol. 14 (2005) 91–99, https://doi.org/10.1361/10599630522774.

[12] M. Faccoli, D. Maestrini, G.P. Marconi, Warm spray applied to steel component repair: experimental study, Surf. Eng. 32 (2016) 707–711, https://doi.org/10.1179/1743294415Y.0000000046.

[13] K. Vinod, R.K. Porwal, Effect of coating on erosion wear: an experimental investigation, {IOP} Conf. Ser. Mater. Sci. Eng. 402 (2018) 12117, https://doi.org/10.1088/1757-899x/402/1/012117.

[14] O. Maranho, D. Rodrigues, M. Boccalini, a. Sinatora, Influence of parameters of the HVOF thermal spray process on the properties of multicomponent white cast iron coatings, Surf. Coatings Technol. 202 (2008) 3494–3500, https://doi.org/10.1016/j.surfcoat.2007.12.026.

[15] M. Mohammadi, S. Javadpour, S. a J. Jahromi, K. Shirvani, a. Kobayashi, Characterization and hot corrosion performance of LVPS and HVOF-CoNiCrAlYSi coatings, Vacuum 86 (2012) 1458–1464, https://doi.org/10.1016/j.vacuum.2012.02.030.

[16] M.R. Ramesh, S. Prakash, S.K. Nath, P.K. Sapra, B. Venkataraman, Solid particle erosion of HVOF sprayed WC-Co/NiCrFeSiB coatings, Wear 269 (2010) 197–205, https://doi.org/10.1016/j.wear.2010.03.019.

[17] J. Saaedi, T.W. Coyle, H. Arabi, S. Mirdamadi, J. Mostaghimi, Effects of HVOF process parameters on the properties of Ni-Cr coatings, J. Therm. Spray Technol. 19 (2010) 521–530, https://doi.org/10.1007/s11666-009-9464-5.

[18] J.M. Miguel, J.M. Guilemany, S. Vizcaino, Tribological study of NiCrBSi coating obtained by different processes, Tribol. Int. 36 (2003) 181–187, https://doi.org/10.1016/S0301-679X(02)00144-5.

[19] N. Serres, F. Hlawka, S. Costil, C. Langlade, F. Machi, A. Cornet, Dry coatings and ecodesign part. 1 - Environmental performances and chemical properties, Surf. Coatings Technol. 204 (2009) 187–196, https://doi.org/10.1016/j.surfcoat.2009.07.012.

[20] Y. Kawahara, Application of High Temperature Corrosion-Resistant Materials and Coatings Under Severe Corrosive Environment in Waste-to-Energy Boilers, J. Therm. Spray Technol. 16 (2007) 202–213, https://doi.org/10.1007/s11666-006-9012-5.

[21] K. Simunovic, T. Saric, G. Simunovic, Different Approaches to the Investigation and Testing of the Ni-Based Self-Fluxing Alloy Coatings—A Review. Part 2: microstructure, Adhesive Strength, Cracking Behavior, and Residual Stresses Investigations, Tribol. Trans. 57 (2014) 980–1000, https://doi.org/10.1080/10402004.2014.927548.

[22] M.J. Tobar, C. Álvarez, J.M. Amado, G. Rodríguez, A. Yáñez, Morphology and characterization of laser clad composite NiCrBSi – WC coatings on stainless steel, 200 (2006) 6313–6317. https://doi.org/10.1016/j.surfcoat.2005.11.093.

[23] S.B. Mishra, K. Chandra, S. Prakash, Erosion-corrosion performance of NiCrAlY coating produced by plasma spray process in a coal-fired thermal power plant, Surf. Coatings Technol. 216 (2013) 23–34, https://doi.org/10.1016/j.surfcoat.2012.09.044.

[24] a.J. López, M. Proy, V. Utrilla, E. Otero, J. Rams, High-temperature corrosion behavior of Ni–50Cr coating deposited by high velocity oxygen–fuel technique on low alloy ferritic steel, Mater. Des. 59 (2014) 94–102, https://doi.org/10.1016/j.matdes.2014.02.027.

[25] N. Bala, H. Singh, S. Prakash, High-temperature oxidation studies of cold-sprayed Ni–20Cr and Ni–50Cr coatings on SAE 213-T22 boiler steel, Appl. Surf. Sci. 255 (2009) 6862–6869, https://doi.org/10.1016/j.apsusc.2009.03.006.

[26] H.S. Grewal, H. Singh, A. Agrawal, Microstructural and mechanical characterization of thermal sprayed nickel-alumina composite coatings, Surf. Coatings Technol. 216 (2013) 78–92, https://doi.org/10.1016/j.surfcoat.2012.11.029.

[27] S. Harsha, D.K. Dwivedi, a. Agarwal, Influence of CrC addition in Ni-Cr-Si-B flame sprayed coatings on microstructure, microhardness and wear behaviour, Int. J. Adv. Manuf. Technol. 38 (2008) 93–101, https://doi.org/10.1007/s00170-007-1072-2.

[28] B. Cai, Y.F. Tan, L. He, H. Tan, L. Gao, Tribological properties of TiC particles reinforced Ni-based alloy composite coatings, Trans. Nonferrous Met. Soc. China (English Ed. 23 (2013) 1681–1688, https://doi.org/10.1016/S1003-6326(13)62648-5.

[29] a. Määttä, U. Kanerva, P. Vuoristo, Structure and tribological characteristics of HVOF coatings sprayed from powder blends of Cr 3C 2-25NiCr and NiCrBSi alloy, J. Therm. Spray Technol. 20 (2011) 366–371, https://doi.org/10.1007/s11666-010-9579-8.

[30] L. He, Y. Tan, X. Wang, T. Xu, X. Hong, Microstructure and wear properties of Al2O3-CeO2/Ni-base alloy composite coatings on aluminum alloys by plasma spray, Appl. Surf. Sci. 314 (2014) 760–767, https://doi.org/10.1016/j.apsusc.2014.07.047.

[31] F. Liu, M. Fang, Z. Huang, Y. Liu, S. Huang, Preparation and mechanical properties of NiCr – Al 2 O 3 – ZrO 2 (8Y) ceramic composites, Mater. Sci. Eng. A. 554 (2012) 1–5, https://doi.org/10.1016/j.msea.2012.05.004.

[32] A.S. Praveen, A. Arjunan, Effect of nano-Al<inf>2</inf>O<inf>3</inf>addition on the microstructure and erosion wear of HVOF sprayed NiCrSiB coatings, Mater. Res. Express. 7 (2019), https://doi.org/10.1088/2053-1591/ab5bda.

[33] Q.Y. Hou, Z. Huang, J.T. Wang, Influence of nano-Al2O3 particles on the microstructure and wear resistance of the nickel-based alloy coating deposited by plasma transferred arc overlay welding, Surf. Coatings Technol. 205 (2011) 2806–2812, https://doi.org/10.1016/j.surfcoat.2010.10.047.

[34] V.A. Andrei, C. Radulescu, V. Malinovschi, A. Marin, E. Coaca, M. Mihalache, C. N. Mihailescu, I.D. Dulama, S. Teodorescu, I.A. Bucurica, Aluminum Oxide Ceramic Coatings on 316l Austenitic Steel Obtained by Plasma Electrolysis Oxidation Using a Pulsed Unipolar Power Supply, Coatings 10 (2020), https://doi.org/10.3390/coatings10040318.

[35] J. Yuan, C. Ma, S. Yang, Z. Yu, H. Li, Improving the wear resistance of HVOF sprayed WC-Co coatings by adding submicron-sized WC particles at the splats' interfaces, Surf. Coatings Technol. 285 (2016) 17–23, https://doi.org/10.1016/j.surfcoat.2015.11.017.
[36] V.H. Hidalgo, J.B. Varela, a.C. Menéndez, S.P. Martínez, High temperature erosion wear of flame and plasma-sprayed nickel-chromium coatings under simulated coal-fired boiler atmospheres, Wear 247 (2001) 214–222, https://doi.org/10.1016/S0043-1648(00)00540-8.
[37] Y.Y. Wang, C.J. Li, a. Ohmori, Influence of substrate roughness on the bonding mechanisms of high velocity oxy-fuel sprayed coatings, Thin Solid Films 485 (2005) 141–147, https://doi.org/10.1016/j.tsf.2005.03.024.
[38] P. Crook, H.N. Farmer, Friction and wear of hardfacing alloys, ASM Handb 18 (1992) 758–765.
[39] R. Kaul, P. Ganesh, S.K. Albert, A. Jaiswal, N.P. Lalla, A. Gupta, C.P. Paul, A. K. Nath, Laser cladding of austenitic stainless steel with nickel base hardfacing alloy, Surf. Eng. 19 (2003) 269–273, https://doi.org/10.1179/026708403322499182.
[40] M. Liu, Z. Yu, Y. Zhang, H. Wu, H. Liao, S. Deng, Prediction and analysis of high velocity oxy fuel (HVOF) sprayed coating using artificial neural network, Surf. Coatings Technol. (2019), 124988, https://doi.org/10.1016/j.surfcoat.2019.124988.
[41] A.S. Praveen, J. Sarangan, S. Suresh, B.H.H. Channabasappa, Optimization and erosion wear response of NiCrSiB/WC–Co HVOF coating using Taguchi method, Ceram. Int. 42 (2016) 1094–1104, https://doi.org/10.1016/J.CERAMINT.2015.09.036.
[42] W. Tillmann, O. Khalil, M. Abdulgader, Porosity Characterization and Its Effect on Thermal Properties of APS-Sprayed Alumina Coatings, Coatings 9 (2019), https://doi.org/10.3390/coatings9100601.
[43] A. G76-18, Standard Test Method For Conducting Erosion Tests by Solid Particle Impingement Using Gas Jets, ASTM International, West Conshohocken, PA, 2018, https://doi.org/10.1520/G0076-18.
[44] V. Chawla, A. Chawla, D. Puri, S. Prakash, P.G. Gurbuxani, B. Singh Sidhu, Hot Corrosion & Erosion Problems in Coal Based Power Plants in India and Possible Solutions-A Review, J. Miner. Mater. Charact. Eng. 10 (2011) 367–385.
[45] H.X. Hu, S.L. Jiang, Y.S. Tao, T.Y. Xiong, Y.G. Zheng, Cavitation erosion and jet impingement erosion mechanism of cold sprayed Ni-Al 2O 3 coating, Nucl. Eng. Des. 241 (2011) 4929–4937, https://doi.org/10.1016/j.nucengdes.2011.09.038.
[46] W.Y. Li, C. Zhang, H. Liao, J. Li, C. Coddet, Characterizations of cold-sprayed Nickel-Alumina composite coating with relatively large Nickel-coated Alumina powder, Surf. Coatings Technol. 202 (2008) 4855–4860, https://doi.org/10.1016/j.surfcoat.2008.04.076.
[47] G. Bolelli, V. Cannillo, L. Lusvarghi, M. Montorsi, F.P. Mantini, M. Barletta, Microstructural and tribological comparison of HVOF-sprayed and post-treated M–Mo–Cr–Si (M=Co, Ni) alloy coatings, Wear. 263 (2007) 1397–1416, https://doi.org/10.1016/j.wear.2006.12.002.
[48] J. Suutala, J. Tuominen, P. Vuoristo, Laser-assisted spraying and laser treatment of thermally sprayed coatings, Surf. Coatings Technol. 201 (2006) 1981–1987, https://doi.org/10.1016/j.surfcoat.2006.04.042.
[49] M... Uusitalo, P.M... Vuoristo, T... Mäntylä, High temperature corrosion of coatings and boiler steels in reducing chlorine-containing atmosphere, Surf. Coatings Technol. 161 (2002) 275–285, https://doi.org/10.1016/S0257-8972(02)00472-3.
[50] B.S. Sidhu, S. Prakash, Evaluation of the corrosion behaviour of plasma-sprayed Ni3Al coatings on steel in oxidation and molten salt environments at 900 °C, Surf, Coatings Technol 166 (2003) 89–100, https://doi.org/10.1016/S0257-8972(02)00772-7.
[51] A. Ul-Hamid, Effect of Y2O3 content on the oxidation behavior of Fe-Cr-Al-based ODS alloys, J. Mater. Eng. Perform. 12 (2003) 87–94, https://doi.org/10.1361/105994903770343529.
[52] G. Wu, N. Li, D. Zhou, K. Mitsuo, Electrodeposited Co-Ni-Al2O3 composite coatings, Surf. Coatings Technol. 176 (2004) 157–164, https://doi.org/10.1016/S0257-8972(03)00739-4.
[53] D. Das, R. Balasubramaniam, M.N. Mungole, Hot corrosion of carbon-alloyed Fe3Al-based iron aluminides, Mater. Sci. Eng. A. 338 (2002) 24–32, https://doi.org/10.1016/S0921-5093(02)00072-2.
[54] C.T. Kunioshi, O.V. Correa, L.V. Ramanathan, High temperature oxidation and erosion–oxidation behaviour of HVOF sprayed Ni–20Cr, WC–20Cr–7Ni and Cr3C2–Ni–20Cr coatings, Surf. Eng. 22 (2006) 121–127, https://doi.org/10.1179/174329406X98403.
[55] S. Kamal, R. Jayaganthan, S. Prakash, S. Kumar, Hot corrosion behavior of detonation gun sprayed Cr3C2-NiCr coatings on Ni and Fe-based superalloys in Na2SO4-60% V2O5 environment at 900 ??C, J. Alloys Compd. 463 (2008) 358–372, https://doi.org/10.1016/j.jallcom.2007.09.019.
[56] G. Sundararajan, The solid particle erosion of metallic materials: the rationalization of the influence of material variables, Wear 186–187 (1995) 129–144, https://doi.org/10.1016/0043-1648(95)07172-5.
[57] N. Gat, W. Tabakoff, Some effects of temperature on the erosion of metals, Wear 50 (1978) 85–94, https://doi.org/10.1016/0043-1648(78)90247-8.
[58] P. Chivavibul, M. Watanabe, S. Kuroda, J. Kawakita, M. Komatsu, K. Sato, J. Kitamura, Effect of powder characteristics on properties of warm-sprayed WC-Co coatings, J. Therm. Spray Technol. 19 (2010) 81–88, https://doi.org/10.1007/s11666-009-9438-7.